energy&fuels

pubs.acs.org/EF Article

Enhanced Oil Recovery from Austin Chalk Carbonate Reservoirs Using Faujasite-Based Nanoparticles Combined with Low-Salinity Water Flooding

Moussa Taleb, Farad Sagala, Afif Hethnawi, and Nashaat N. Nassar*

Cite This: https://dx.doi.org/10.1021/acs.energyfuels.0c02324 Read Online

ACCESS | Metrics & More | Article Recommendations | Supporting Information

ABSTRACT: Recently, the application of nanoparticles for enhancing oil recovery (EOR) in carbonate reservoirs has received great attention from various researchers across the oil and gas industry. In contrast to sandstone reservoirs, carbonates are naturally neutral wet or preferentially oil wet and, therefore, the recovery of oil from these reservoirs by waterflooding techniques is relatively low and inefficient. Hence, the addition of chemical agents can modify rock wettability and increase the efficiency of the waterflooding process. The role of nanoparticles and their implementations in the field of oil recovery has been highlighted by many researchers in the past, due to their attractive features and characteristics. However, choosing the appropriate nanoparticles is not the only limiting factor to guarantee better performance in EOR but also depends on their stability and dispersion under aqueous conditions. Accordingly, many metal oxides or silicate-based nanomaterials have been subjected to surface modifications, following some complex and costly ineffective functionalization steps before their application. In this study, novel and stable nanomaterials of faujasite were synthesized at mild conditions without following any surface modification steps to alter the wettability of Austin Chalk carbonate rocks from oil wet to strongly water wet in the presence of low-salinity water (LSW). The synthesized nanoparticles were well characterized by scanning electron microscopy (SEM), transfer electron microscopy (TEM), X-ray diffraction (XRD), dynamic light scattering (DLS), and ζ potential to confirm their surface identity, functionality, morphology, and stability. The prepared nanofluids from the synthesized nanoparticles were tested in comparison to brine for their EOR efficiency in carbonate cores. The EOR performance was investigated by interfacial tension (IFT), contact angle, spontaneous imbibition, and displacement tests. The results showed that, compared to formation brine and LSW, the formulated nanofluid could notably alter the rock wettability from strong oil wet to strong water wet. To confirm this, a core-flooding test was performed, which further reiterated the capability of these nanofluids as effective EOR agents in hydrocarbon carbonate reservoirs by recovering an additional 9.6% of OOIP. Consequently, on the basis of the obtained findings, these faujasite-based nanofluids provide a prospect of being applied in EOR in carbonate formations.

1. INTRODUCTION

With the steady increase in global population and economic growth of developing countries, energy demand is expected to grow gradually within the upcoming decades. According to BP's "Energy Outlook 2035", global energy consumption is expected to rise by 41% from 2012 to 2035, with 95% of that growth being attributed to demand from emerging economies.[1,2] Furthermore, the International Energy Agency (IEA) estimates that global demand will grow by 7.3 million Barrels/Day through 2022, with this growth being influenced by the automotive, airline, and chemical industries.[3] Although this forecast gives a positive outlook for the future of energy demand, there are still many important challenges facing the oil and gas industry. Some of these include oil price volatility, greenhouse gas emissions, high production costs, unconventional oil and gas exploitation, and the emergence of alternative energy sources.[4] These challenges have motivated industry partners and academics to pioneer innovative methods to increase oil and gas production to serve the global energy demand in a more environmentally friendly and cost-efficient manner. Enhanced oil recovery (EOR) is one of the methods used to tackle these issues, yet according to the IEA, it currently only accounts for 2% of the global oil supply.[5] However, the agency expects EOR production to almost double in the upcoming decades. This is attributed to the anticipated demand from mature production provinces to pursue efforts to maintain production or slow declines in productions. Numerous experimental works have been published discussing the role of chemical agents in the wettability alteration of the porous medium.[6,7] Chemical enhanced oil recovery (CEOR) utilizing nanotechnology is a novel technique that aims to tackle some of the challenges associated with extracting residual oil from reservoir rocks after primary and secondary production. A major field application using this technique has not yet been conducted; however, it has been demonstrated that the application of nanotechnology within the oil and gas industry has great potential in terms of

Received: July 12, 2020
Revised: September 20, 2020

improving exploration, production, reservoir characterization, drilling, and completions and may serve as an appropriate alternative for enhancing oil recovery over tradition chemical EOR methods.[8−11] Nanotechnology in general terms is used to describe the application and effective use of material that is less than 100 nm in size, at least in one dimension.[12] Thus, it has been applied to a plethora of disciplines including physics, biology, chemistry, and many engineering subfields. The role of nanoparticles in this field is still in its infancy and progressively has attracted the attention of many researchers in recent decades, due to their unique physical and chemical properties.[8,13] Some of these properties include the high surface area to volume ratio, optical transparency, chemical catalysis, electrical conductivity, and mechanical strength.[13−20] Although several types of nanoparticles, such as $CaCO_3$, SiO_2, TiO_2 Al_2O_3, carbon nanotubes (CNT), graphene oxides (GO), nanopyroxene, etc., have been proposed as effective EOR agents, there remains a challenge in terms of nanoparticle aggregation.[21,22] To overcome this challenge, the surface of the nanoparticles is modified by anchoring certain types of polymers, surfactants, or silane groups to improve the surface electrostatic repulsion.[23,24] Yet, it may not be convincing enough for operators to favor these modified agents over conventional EOR agents due to the complexity of the procedure and associated costs. Thus, many researchers, with endless pressure, are continuously seeking innovative nanomaterials that can be thermodynamically stable without following functionalization procedures. Moreover, nanomaterials can be combined with other traditional methods such as polymers, surfactants, or alkaline flooding to produce the trapped oil from the reservoir.[11,25] Despite the noticeably increasing interests of nanoparticle applications in EOR, there still exists some challenges that limit their full adoption in the industry such as stability and aggregation. Typically, because of harsh reservoir conditions such as temperature and salinity, nanoparticles normally aggregate due to an imbalance between the repulsive and attractive forces.[26,27] Nanoparticle agglomeration results in a reduction of the effective surface area to volume ratio, which impacts the overall performance and behavior of the nanofluids, especially in these harsh conditions.[28] Nonetheless, adding nanoparticles to brine with a low ionic strength helps enhance their stability in solution and improve their performance. Over the past decade, low-salinity water flooding (LSWF) has been recognized as the least expensive new alternative technique for EOR applications. Moreover, laboratory experiments and field trials over the past decade have shown that LSWF can recover additional oil.[29,30] The postulated mechanism of LSWF includes wettability alteration toward water wet from intermediate/oil wet, IFT reduction, and saponification.[29,31,32] Furthermore, fine particle migration has been found to take place during LSWF.[33] It was also evidenced that, because of the changes to the surface ζ potentials, attractive forces between mobilized fine-grained particles and static grain surface can be reinforced using nanoparticles.[24,34] Notwithstanding the comprehensive studies of LSWF, however, the role of nanoparticles when dispersed in brine with an optimum ionic strength for EOR application in carbonate reservoirs is a new field of study in its infancy stage that requires further investigation. Silica−alumina or zeolite nanoparticles have been widely used for various applications since they are environmentally safe materials, stable, and owning to their excellent surface properties.[35] Thus, they are an attractive material for EOR applications. Zeolites are low-density crystalline aluminosilicates that are composed of regular and well-defined pore sizes and shapes. The structure of zeolite is combined with hydrophilic/hydrophobic, and their porous nature renders them as useful shape-selective molecular sieves and hosts for various guest molecules (organic and inorganic).[36] Numerous efforts have been made to develop a synthesis procedure of zeolites with nanometer dimensions to enhance the accessibility of reactant molecules.[35] With a high accessible surface, the structure can provide a fast diffusion in adsorption and ion-exchange processes. In addition to the regular micropores, the zeolite-based nanoparticles are characterized by having meso- and macropores due to the homogeneity of size and morphology of the closely packed crystals.[35] Accordingly, zeolite in nanoscales are colloidal stable under aqueous medium with different concentrations and do not agglomerate with time. Wijayanto et al.[37] recently synthesized and applied aluminum silicate to enhance the oil recovery in sandstone cores. However, the obtained nanomaterials had a lower surface area (80 m^2/g) and a large particle size (90 nm). The formulated nanofluid at a concentration of 20 ppm showed a noticeable aggregation, which could result in pore throat blockage. For that purpose, an effective synthesis protocol for the alumina−silicate nanoparticle should be used to generate lower sizes and high-stability nanoparticles to provide better performance in EOR. The synthesis of zeolite-based nanoparticles can be accomplished by using a one step-hydrothermal method in the presence of certain mesopore and morphology modifiers under well-tuned conditions especially with a low-crystalline-size domain and high external surface area. For instance, the faujasite (FAU) type zeolite nanomaterials are formed through the use of organic or extra inorganic morphology-directing templates or agents. The FAU nanomaterials with low-crystalline-size domains are characterized by owing a considerable increase of their external surface and the associated properties that permit us to explore the adsorption and reaction of bulky molecules that do not normally interact with the microporous nanozeolites.[35] Herein, we present one novel synthesis method for high surface area and highly stable FAU nanoparticles without using morphology modifiers or stabilizing agents, which could potentially serve as an economically viable, environmentally friendly, and more efficient displacing agent when applied in carbonate reservoirs for EOR application. The generated nanoparticles were well-characterized using an array of characterization methods. Then, the FAU nanomaterials were used to generate stable nanofluids using a low-salinity brine. The formulated nanofluids were tested in comparison to synthetic formation brine and low-salinity water alone for their EOR efficiency in carbonate cores. The EOR performance was investigated by interfacial tension (IFT), contact angle, spontaneous imbibition, and displacement tests. The results showed that compared to brine alone, nanofluids could notably alter the rock wettability from oil wet to water wet. To confirm this, a core-flooding test was performed that further reiterated the capability of these nanofluids as effective EOR agents in hydrocarbon carbonate reservoirs by recovering an additional 9.6% in comparison to formation brine flooding at the tertiary stage. This study provides insights on the underlying chemistry of LSWF when combined with nanoparticles for EOR applications in carbonate reservoirs at different salinities. Furthermore, it outlines an inexpensive technique for mobilizing trapped oil by improving the performance of conventional LSWF by integration of faujasite-based nano-

https://dx.doi.org/10.1021/acs.energyfuels.0c02324
Energy Fuels XXXX, XXX, XXX−XXX

Table 1. Properties of Crude Oil Sample Considered in This Study

viscosity at 25 °C	TAN (mg KOH/g)	asphaltene (wt %)	saturates (wt %)	aromatic (wt %)	resin (wt %)	density (g/cm^3)	API (deg)
74.0	0.71	9.6	12	58.4	20	0.94	17.4

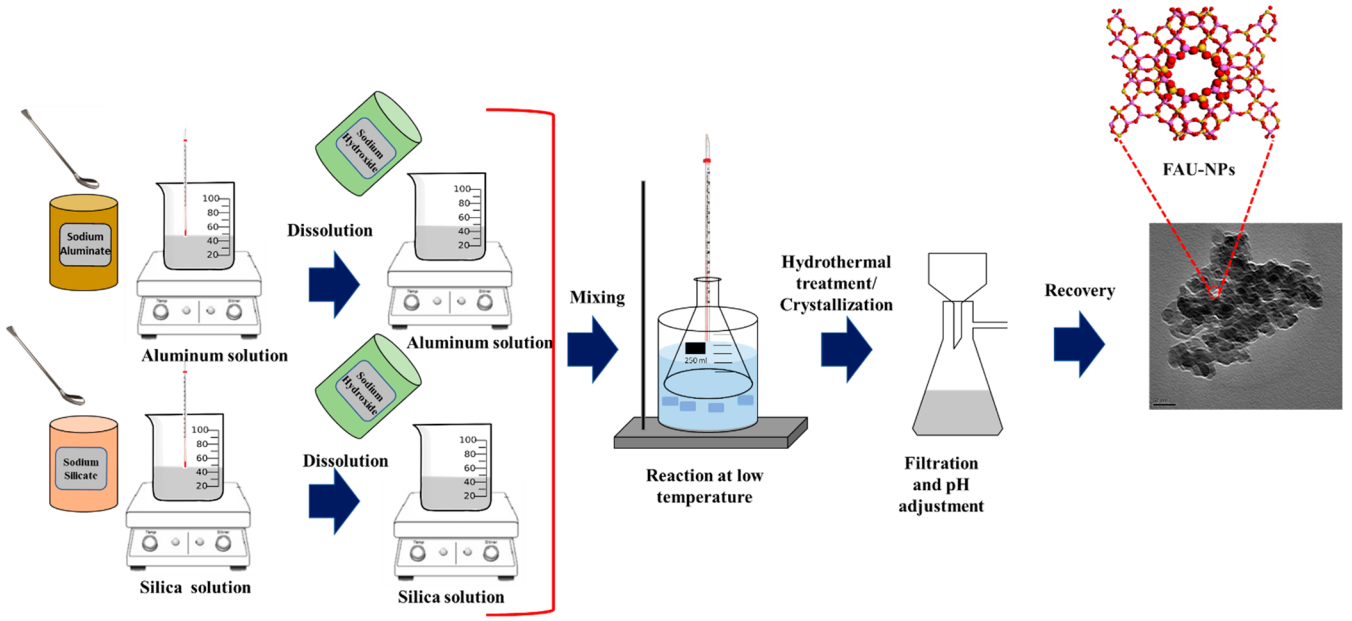

Figure 1. Schematic illustration of the synthesis procedure of Y-zeolite of FAU nanoparticles.

particles when dispersed in LSW, as one of the inexpensive techniques of reducing trapped oil.

2. MATERIALS AND METHODS

2.1. Materials. Rock mineralogy impacts the performance of LSW in carbonate reservoirs; therefore, to determine the rock mineralogy, X-ray diffraction (XRD) experiments were performed before conducting the wettability and flooding tests. The results from the XRD tests showed that the rock consisted of mainly calcite, as shown in Figure S1 of the Supporting Information. The X-ray analysis was performed using a Rigaku ULTIMA III X-ray diffractometer with Cu Kα radiation as the X-ray source. The scans were done in the range 3°−90° of 2θ using a 0.05° step and a counting time of 1.0°/min, operating at 40 kV and 44 mA to obtain the full diffractogram for the analyzed materials. The samples were placed in a Rigaku zero background sample holder model 906163 (10 mm × 0.2 mm Well Si510) for their analysis to avoid any contribution of amorphous material from the conventional glass sample holders. Sodium chloride (NaCl, 99%), magnesium chloride ($MgCl_2$, 99%), calcium chloride ($CaCl_2$, 99%), sodium silicate (Na_2SiO_3, 99 wt % purity), NaOH (99 wt % purity), sodium aluminate (Al_2O_3, Na_2O), *n*-heptane, and toluene (99%) were all purchased from VWR and used as received. The fluid density, pH, and viscosity were measured using a pycnometer, pH meter (VWR), and Brookfield viscometer, respectively. The source of oil used in this study was an acidic crude oil sample provided by an oil company based out of Calgary, Canada.

Table 1 outlines the properties of the crude oil used in this study. The viscosity of the oil as a function of temperature is provided in Figure S2. For testing the oil recovery, Austin Chalk carbonate cores (as seen in Figure S3) originating from the Upper-Cretaceous formation with a permeability range of 8−15mD and a porosity range of 25%−27% were selected and provided by Kocurek Industries Inc., Caldwell, TX.

2.2. Fluid Formulations. Synthetic brine (SB), representing formation brine (FB), was prepared from NaCl (2 wt %), $CaCl_2$ (0.2 wt %), KCl (0.2 wt %), $MgCl_2$ (0.1 wt %), and deionized water to represent formation water (FW) with approximately 2.5 wt % (25000) (ppm). Brine with a lower-salinity (without divalent ions) (LSW) solution was selected by performing ζ potential measurements as detailed in the following. When designing the optimum water composition for LSW in carbonates, it is important to determine the ζ potential at both the rock−water and oil−water interfaces. If the oil−water interface carries negative charges, modification of the injected brine composition to yield a more negative ζ potential on the rock surfaces results in improved oil recovery and is desirable. Due to the ionization of the chemical groups in the presence of various aqueous ionic solutions, it has been reported that surface charges exist at the fluid−fluid and fluid−rock interfaces.[38] ζ potential measurements, with various salinity levels, were used to determine the electrical charges at the interfaces of fluid−rock and fluid−fluid, which control the stability of the water film and the rock wettability, hence EOR/IOR. We thus measured the ζ potential at interfaces of oil/brine and brine/rock using the Malvern Zetasizer ZS Nano series supplied by Malvern Instruments Ltd. (Westborough, MA, USA). ζ potential measurements were performed in a pH range of 6−7, typical for carbonate reservoirs. To prevent brine evaporation at higher temperatures and given the stability of ζ potential measurements at ambient conditions, all ζ potential measurements were performed at 25 °C. ζ potential measurements were performed by mixing 0.5 g of the carbonate crushed rock sample with different brine compositions such as NaCl 0 (DIW), 500, 1000, 2000, 3000, 5000, 10000, 20000 ppm and FW (25000 ppm) containing divalent cations Ca^{2+} and Mg^{2+}, as detailed previously. The brine composition that resulted in the highest ζ potential was selected to be the dispersant for FAU for this study. All measurements were repeated in triplicates, and the standard deviation error of the mean was reported.

2.3. Synthesis of Faujasite Nanoparticles and Nanofluid Preparation. *2.3.1. Synthesis of Faujasite Nanoparticles.* Faujasite-based nanoparticles (FAU) were synthesized following a hydrothermal method as illustrated schematically in Figure 1. Two base solutions were generated to form the FAU nanomaterials. The first basic solution named as (BS 1) was prepared by dissolving 5.151 g of sodium aluminate into 29 g of deionized water under magnetic stirring at 300 rpm. After a clear solution was formed, 3.057 g of

https://dx.doi.org/10.1021/acs.energyfuels.0c02324
Energy Fuels XXXX, XXX, XXX−XXX

NaOH was added to the solution and stirred again until it was transparent. The same method was used to prepare the second basic solution (BS 2), but instead, 85.297 g of sodium silicate was diluted with 28 g of deionized water along with 10.104 g of NaOH. Both solutions were stored in the fridge and cooled to a temperature of 15 °C or less after preparation. After cooling the two solutions in the fridge, a glass beaker containing BS 2 was placed in a cold water−ice tube under magnetic stirring at 300 rpm and BS 1 was slowly added drop by drop. A clear solution was always obtained, and the temperature was monitored constantly to ensure that it did not drop below 20 °C. After BS 1 was completely added to BS 2, the mixture was poured into a 250 mL polypropylene bottle and capped tightly to allow the solution to age at room temperature for 24 h. After aging, the plastic bottle was set inside a glass beaker and placed in an oven at 50 °C for 48 h to allow the mixture to crystallize. Subsequently, the beaker containing the plastic bottle was removed and left to cool down to room temperature for some time. Finally, the clear solution was transferred to a filter funnel containing a porous filter paper as the base. The product was continuously washed and filtered for several hours with deionized water until the pH of the washed water was close to 8−9. Afterward, the solid remaining (approximately 5 g) was dried at room temperature overnight ready for further usage.

2.3.2. Synthesis of Nanofluids. Three fluids were prepared for the comparative study as shown in Table 2, which presents the fluid properties. Brine with a lower salinity without divalent ions (LSW) solution was selected on the basis of ζ potential measurements from sodium chloride (NaCl) at 0.2 wt % (2000 ppm) and deionized water as a dispersing medium for the nanoparticles. For comparison, a FAU-based nanofluid solution was prepared by dispersing 50, 100, and 200 ppm of the prepared nanoparticles into either 2000 ppm LSW or FW solutions. To ensure proper dispersion of the nanoparticles within the mixture, the nanofluid suspension was agitated in an orbital shaker at 250 rpm. Afterward, the solutions were ultrasonicated in an ultrasonic bath for 60 min.

Table 2. Properties of the Synthesized Nanofluids

prepared fluid	density (g/cm^3)	pH
FW	1.013 ± 0.001	8.5
LSW (2000 ppm)	0.998 ± 0.001	6.7
50 ppm	0.996 ± 0.001	7.4
100 ppm	0.997 ± 0.001	7.8
200 ppm	0.999 ± 0.001	7.6

2.4. Nanoparticle and Nanofluid Characterization. The prepared FAU nanoparticles were characterized using an array of characterization techniques to determine their morphology, crystalline size, and surface area. Morphology and surface topology were obtained by a JEM-2100 scanning electron microscope (SEM) of JEOL, Ltd. The crystalline domain size was determined through X-ray diffraction (XRD), using a Rigaku ULTIMA III X-ray diffractometer with Cu Kα radiation as the X-ray source. The scan was operated at 40 kV and 44 mA to obtain the full diffractogram for the nanoparticles and was performed in the range 3°−90° of 2θ using a 0.05° step and a counting time of 1.0°/min. The XRD data was processed using the PDXL software from Rigaku, and the crystalline sizes were calculated using the Scherrer equation. Furthermore, the surface area and porosity were approximated by using the TriStar II 3020, Micrometrics Instrument Corporation, Norcross, GA, which uses the Bruneur−Emmet−Teller (BET) equation to estimate the surface area.

For nanofluid stability and characterization, dynamic light scattering (DLS) and ζ potential analysis were used to determine the average hydrodynamic size distribution and stability of the particles in the brine solution. This was conducted on a variety of nanofluids with varying concentrations to determine the most optimal concentration to use in the study. To accomplish this analysis, a Zetasizer Nano Series system from Malvern Instruments Ltd., Westborough, MA, USA was utilized.

2.5. Interfacial Tension (IFT) Measurements. Interfacial tension measurements (IFT) were conducted on the prepared nanofluids to evaluate their role in reducing the IFT between oil and brine. The measurements were performed using Attention PD 200 from Biolin Scientific, Finland. The Attention PD 200 is a computer-controlled module that enables a controlled perturbation (such as sinusoidal oscillation, triangular, and square perturbation) for pendant drops or bubbles and, thus, study of dilatational interfacial rheology. The perturbation is achieved with a piezo pump enclosed in a chamber. The piezo pump is driven through pulse modulating electronic units. This involved a dynamic study of FAU-based nanofluids of different concentrations at the oil−water interface. The equilibrium surface tension was measured with optical tensiometers using optical tensiometry to investigate the surface and interfacial tension of the nanofluids. In this method, the shape of a liquid drop hanging from a syringe tip was determined from the balance of forces that includes the surface tension of the liquid. The surface or interfacial tension at the liquid interface was related to the drop shape through eq 1,

$$\gamma = \Delta\rho g R_0 / \beta \quad (1)$$

where γ is the surface tension, $\Delta\rho$ is the density difference for the fluids at the interface, g is the gravitational constant, R_0 is the radius of drop curvature at the apex, and β is the shape factor; the shape factor can be defined through the Young−Laplace equation.[39,40]

2.6. Preparation of Oil-Wet Core Plugs and Oil Presaturation. Generally, most carbonate rocks are considered intermediate wet or oil wet in their original state because they naturally adsorb the acidic components in the crude oil onto their surface. Furthermore, the bonding energy between the polar components in oil and carbonates is reportedly higher than what is observed in sandstones, which could also explain their initial wettability state.[41] However, since the Austin Chalk cores used for this study were commercially purchased, a procedure to ensure oil wetness in the cores was employed. The cores were initially cut into uniform cylindrical columns with a length of 4 cm and a diameter of 2.54 cm, as shown in Figure S3 of the Supporting Information. Afterward, the cores were cleaned using a Soxhlet apparatus, which is consistent with the API standard for removing hydrocarbons and salts from a core sample.[42] Then, the cleaned cores were dried in an oven at 70 °C for 24 h, and their weights afterward were measured (dry weight). Subsequently, the carbonate cores were saturated with oil using a vacuum pump for 3−6 h. Moving on, the cores were completely submerged in a 10 v/v % solution of *n*-heptane and crude oil and were left to age at 50 °C for 3 weeks. Following the aging process, the oil-saturated cores were weighed, and the weight difference between the dry and wet states was used to determine the volume of the oil initially in place (OOIP) in each core.

2.7. Contact Angle Measurements and Spontaneous Imbibition Tests. For contact angle measurements, the small carbonate substrates shown in Figure S4 of the Supporting Information were cut from the core samples and then aged in oil for approximately 10 days to alter their initial wettability. The oil aged substrates were submerged into the prepared nanofluids and brine for 48 h at room temperature. The contact angle measurements between the carbonate substrates and brines or nanofluids were performed using an Attention from Biolin Scientific, Finland, with an accuracy of ±5°. The angles were then analyzed to quantify the effect of the nanofluid on wettability alteration within the carbonate substrates at the test temperature of 70 °C. Moreover, another technique used to study the wettability alteration within the oil-wet carbonate core samples was the spontaneous imbibition test. Each oil-saturated core sample was immersed in an imbibition Amott cell containing either FW (for comparison), LSW, or FAU-nanofluid. The produced oil volume from the cores due to the fluid imbibition was recorded, expressed as a percentage of original oil in place (% OIIP), and was plotted versus time for the different fluids used. The imbibition experiments were also performed at 70 °C.

https://dx.doi.org/10.1021/acs.energyfuels.0c02324
Energy Fuels XXXX, XXX, XXX−XXX

2.8. Displacement Test. The core-flooding tests aimed to reveal the capability of the FAU-based nanofluids to recover additional oil in the carbonate cores in comparison to traditional water flooding. Figure 2 shows the schematic diagram of the core-flood setup. The

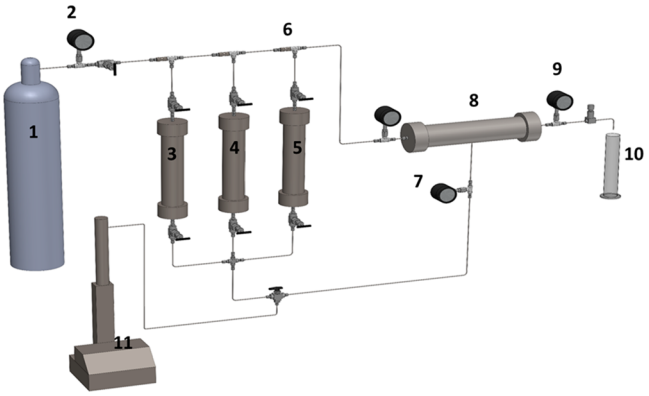

Figure 2. Displacement test diagram: (1) carbon dioxide cylinder, (2) manometer gauge, (3–5) transfer cells for oil, brine, and nanofluids, respectively, (6) valves, (7) overburden pressure gauge, (8) core holder, (9) pressure transducer, (10) collector, and (11) ISCO pump.

experimental procedure and equipment used for this test followed the same method outlined by Sagala et al.[43,44] Based on the stability and imbibition tests, the optimal nanofluid concentration of 50 ppm was selected for the core-flooding experiments in the tertiary flooding mode using three core plugs C1, C2, and C3. Before testing, the core was inserted into a rubber sleeve and mounted into the core holder. CO_2 gas was injected through the sample at a constant low pressure (~250 psi) for 1 h to displace any trapped air in the rock pores. Afterward, a vacuum pump was installed and operated for 6 h to ensure that the gas remained trapped inside the flowlines and core sample was eliminated. The core holder outlet was connected to a back-pressure regulator (BPR) to provide the required pore pressure for core-flooding experiments. The core sample was saturated with brine at a confining pressure of 1000 psi, a pore pressure of 500 psi, and a constant injection rate of 0.2 mL/min. The injection rate was selected to mimic typical reservoir velocities (corresponding to a Darcy velocity of 1 ft/day).[45] This yielded an average steady pressure drop, which was then used to calculate the absolute permeability through Darcy's law. Furthermore, the core was saturated with oil until the water cut was under 1%, and the system was left to age for 24 h to simulate the reservoir equilibrium conditions and estimate the S_{wir}. This set the stage for the tertiary fluid-flooding mode. Then, the FW, LSW, or nanofluid was injected into the core in the tertiary mode and additional produced oil from the core was recorded in a two-phase separator tube. The experiments were conducted at 70 °C.

3. RESULTS AND DISCUSSION

3.1. Nanoparticle Characterization. FAU nanoparticles were successfully synthesized by the hydrothermal method at room temperature, and their structural identity, crystalline size, surface area, and stability in the aqueous medium were confirmed. Figure 3a,b shows optical SEM and TEM images of the prepared FAU nanoparticles. The nanocrystalline material

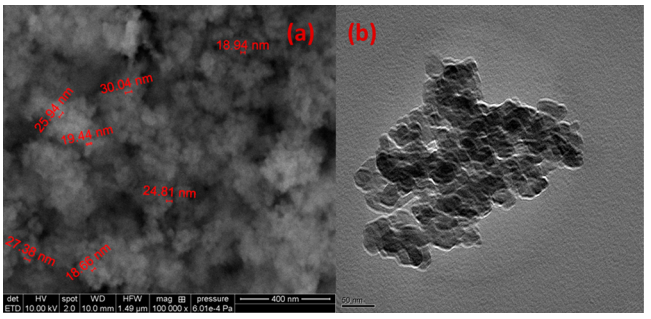

Figure 3. (a) SEM and (b) TEM images obtained for the FAU nanoparticles.

is made up of coarse fused crystals of uniform size and spherical shape with an average diameter of 24 nm.

Figure S5 shows the X-ray diffraction (XRD) patterns of the synthesized FAU nanoparticles. As shown, the obtained patterns for the prepared material confirmed the formation of a sodium-faujasite (Na-FAU)-based material, such that the obtained XRD pattern fits with the reported signals for faujasite, $Na_{71}(Si_{121}Al_{71})O_{384}$, 1507214 in the 2015 ICDD (International Centre for Diffraction Data) database included in the program JADE (Materials Data XRD Pattern Processing Identification and Quantification). As the Si/Al ratio is higher than 1.5, this suggests that the obtained Na-FAU is a Y-type zeolite.[46] Thus, it is expected that the hydrophobicity of FAU will be decreased, since a higher content of Al, with respect to Si, leads to a less hydrophobic surface.[47] This will assist in attracting the FAU nanoparticles to both polar and nonpolar compounds; thus, it will present at the interface between oil and water and it will also stabilize a water film on the mineral surface that would lead to wettability alteration. Having such a spectrum indicates that FAU nanoparticles have been successfully synthesized and the low broadening observed in the patterns indicates the formation of materials with very small crystalline domain sizes. Furthermore, the BET surface area analyzer showed that the synthesized material had a total surface area of 380 m^2/g. Assuming the material has spherical particles, the particle size (d) in nm could be determined by the equation $d = 6000/(SA\ \rho)$,[48] where SA is the experimentally measured specific surface area (m^2/g) and ρ is the density of FAU particles (1 g cm^{-3}). The calculated diameters from the previous equation were around 20 nm, which is approximately similar to that obtained by SEM and XRD. This confirms that the generated nanomaterials had a low tendency for agglomeration. Moreover, the pore size distribution (PSD) has been plotted to show the Y-type FAU zeolite having a hierarchical structure, as shown in Figure S6 in the Supporting Information.

3.2. ζ Potential Measurements. Figure 4 shows the measured ζ potential between the crushed carbonate particles and brine with different salinities. ζ potential measurements were performed to understand the interactions between brine–rock and oil–brine at various salinities and how it can affect

Table 3. Physical Properties of Core Samples

core ID	diameter (cm)	L (cm)	initial fluid	PV (mL)	bulk volume (Vb)(mL)	Φ (%)
C1	3.81	4.7	FB	14.26	53.55	26.63
C2	3.81	4.8	LSW	14.65	54.69	26.78
C3	3.81	4.8	FAU	15.00	54.41	27.42

https://dx.doi.org/10.1021/acs.energyfuels.0c02324
Energy Fuels XXXX, XXX, XXX–XXX

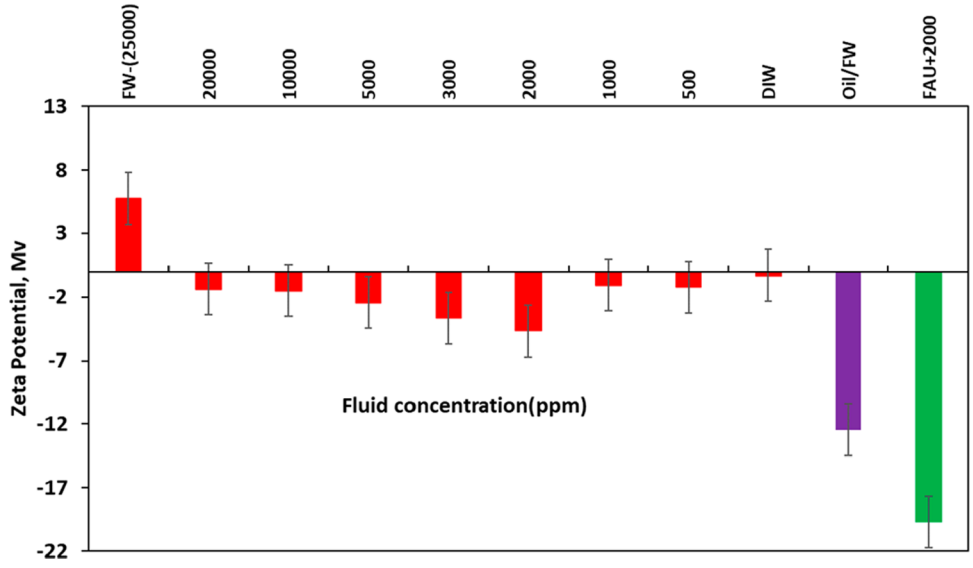

Figure 4. ζ potential measurements of carbonate particles in the presence of different brine/oil solutions.

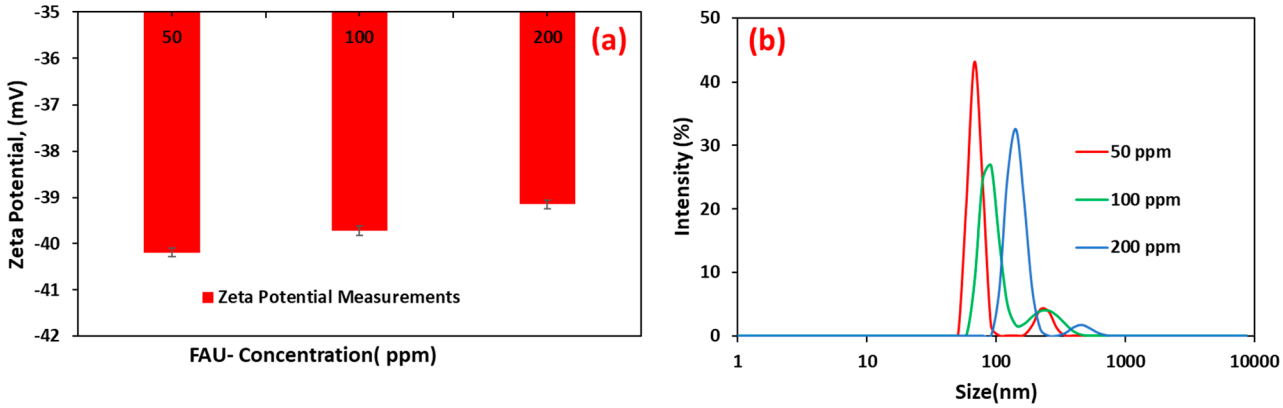

Figure 5. (a) ζ potential measurements and (b) DLS measurements for different concentration of nanoparticles.

the wettability and improve oil recovery. During LSW flooding in carbonate reservoirs, improved oil recovery can be observed only if the change in brine composition gives a ζ potential at each interface that has the same polarity. Therefore, an electrostatic repulsive force acts between the interfaces and hence stabilizes a water film on the mineral surface, maintaining the initial wettability. Therefore, a brine that gives the highest ζ potential can provide a better magnitude of this repulsive force at the interface. The measured ζ potential of the sample in FW was +5.74 mV, consistent with previously published data that reports the ζ potential of formation brine in carbonates normally in the range of <10 mV,[49] and then gradually became more negative but in a small magnitude (<5 mV) as the brine concentration decreased. These results are also consistent with the previous findings of natural carbonates.[49−51] Using formation brine, the oil−brine interface resulted in a ζ potential of −12.45 mV; this negative ζ potential at the interface especially in carbonates reflects an oil-wet condition according to Jackson and Vinogradov.[51] The ζ potential polarity at the oil−brine interface plays a significant role in controlling whether improved oil recovery will occur during the LSW injection. Normally, the hypothesis is that EOR will occur during LSWF when the electrostatic repulsion between the oil−brine and rock−brine interfaces increases as a result of the change in brine composition during brine flooding, which was the obtained trend for our ζ potential measurements for the used rock sample. Therefore, the brine salinity (2000 ppm) that resulted in the highest ζ potential and was expected to give the highest repulsive force and result in additional recovery was selected as a dispersing medium for the FAU nanoparticles. Moreover, the addition of FAU nanoparticles with 0.005 wt % to LSW increased the ζ potential to −19.7 mV. This increment can significantly improve the performance of LSW during EOR due to the formation of a stable water film at the rock interface.

3.3. Nanofluid Characterization. The reason for selecting the FAU framework mentioned in this study was due to the hypothesis that the addition of aluminum assists in maintaining dispersibility and stability without the need for surface modification, unlike other forms of nanoparticles commonly used in EOR. Moreover, the synthesis protocol of FAU offers options for scalability since they can be prepared at mild conditions. Thus, it was expected that FAU would be stable when dispersed in the brine solutions with limited aggregation. Nanofluid solutions containing FAU were formulated by dispersing 50, 100, and 200 ppm in 2000 ppm brine. The solutions were subjected to agitation using an orbital shaker followed by sonication in an ultrasonic bath. It

https://dx.doi.org/10.1021/acs.energyfuels.0c02324
Energy Fuels XXXX, XXX, XXX−XXX

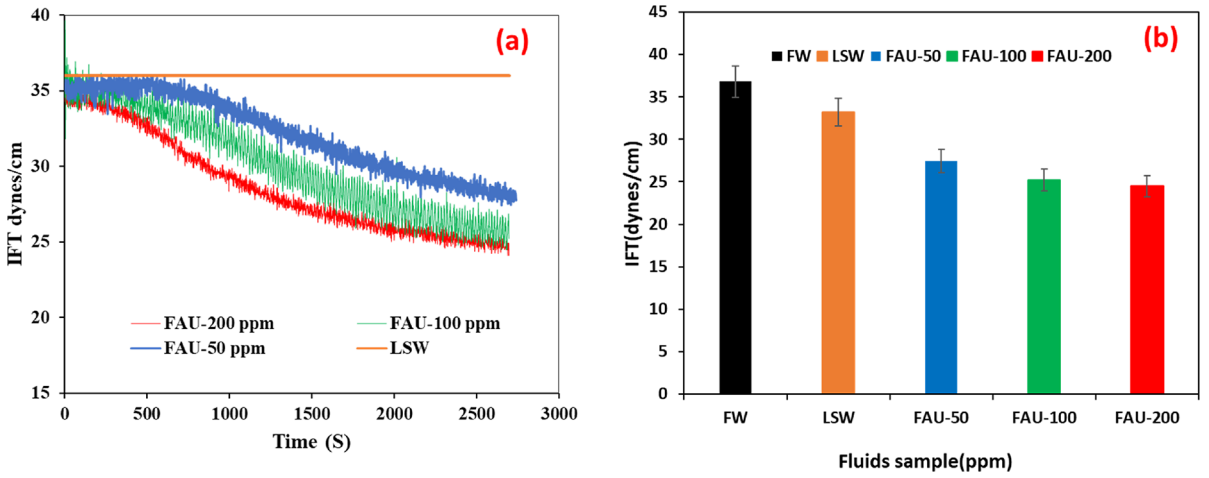

Figure 6. IFT measurements for LSW with different concentrations of nanoparticles (a) dynamic and (b) at equilibrium.

was evident visibly that there was a proper dispersion of the nanoparticles in the fluid as there was no aggregation or precipitation present even after leaving the solutions for several hours. For a more conclusive evaluation of surface stability, ζ potential and DLS measurements were performed for the FAU-based nanofluids. Figure 5a shows the average ζ measurements of the FAU-based nanofluids for the different concentrations. The value of ζ is representative of stability; a lower ζ value (typically less than −30 mV) indicates more stability of the nanofluid and less tendency of flocculation and precipitation.[43,52] As seen, ζ values for the nanofluids with different FAU concentrations are all less than −30 mV. However, as the concentration increases, the ζ value tends to increase because nanoparticles tend to start aggregating. A similar trend of nanoparticle flocculation as the concentration increases was also depicted on the DLS trend in Figure 5b. This indicates that an optimum concentration of nanoparticles is required to formulate stable nanofluids to be used in the oil recovery application.

3.4. Interfacial Tension Measurements. Interfacial tension (IFT) measurements were conducted for the prepared fluids to evaluate their role in reducing the IFT between oil and formation water (FW), water with low ionic strength, or the prepared nanofluids using the pendant drop technique at ambient conditions. The IFT measurements were conducted while varying the time and concentration, as shown in Figure 6a,b. On the basis of the obtained results, neither time nor concentration had a significant effect on the IFT reduction at ambient conditions. Therefore, for this particular nanofluid and the crude oil used in this study, IFT reduction is not among the governing mechanisms of EOR. Since IFT reduction affects the oil displacement by increasing the capillary number, a higher capillary number can only be achieved when a significant reduction in IFT occurs, for example, a reduction of capillary number from 10^{-5} that exists during water flooding to 10^{-3} is required to have a significant oil displacement during EOR.[53,54] Table 4 shows the obtained capillary number with and without nanoparticles N_{C1} and N_{C2}, respectively. From the calculated capillary numbers, it is noticeable that, although nanoparticles could alter the wettability to a stronger water wet conditions, still there was no change in the capillary number since the IFT was still high. The presence of the nanoparticles in the solution slightly decreased the IFT between the oil and brine by approximately

Table 4. Capillary Numbers with Nanoparticles N_{C1} and without Nanoparticles N_{C2} Obtained in This Study

fluid	σ (dyn/cm)	θ (deg)	N_{C1}	N_{C2}
FW	36.8	147.0	2.9×10^{-5}	3.4×10^{-5}
LSW	27.8	61.9	3.8×10^{-5}	8.1×10^{-5}
LSW+FAU	23.7	53.0	3.9×10^{-5}	6.6×10^{-5}

28% (from ∼36.8 to ∼24.5 dyn/cm). This reduction is likely due to the adsorption of large oil molecules, like asphaltenes, onto the nanoparticle surface, which prevents the precipitation of asphaltenes on the interface between the two fluids.[18] Although there was a noticeable reduction in the IFT due to the presence of the nanoparticles, it is still not significant to mobilize residual oil since the value is still relatively high on the basis of the capillary desaturation curve.[54]

3.5. Contact Angle and Spontaneous Imbibition Tests. *3.4.1. Contact Angle Measurements.* As mentioned in the previous sections, carbonate reservoirs are naturally neutral wet or preferentially oil wet, in contrast to sandstones. Nevertheless, the Austin Chalk substrates were aged in oil to ensure complete oil wetness, after which contact angle measurements were conducted. Figure 7 shows the oil droplet contact angle measurements that were obtained by measuring the aged substrates in formation water (panels (a) and (b) in the presence of brine with low ionic strength and panel (c) in the presence of FAU nanofluids). It is worth noting here that a 50 ppm FAU concentration was selected for the contact angle measurements on the basis of the stability and IFT findings. As seen from Figure 7a, the oil drop contact angle of the substrate was (33° ± 2), indicating strong oil-wet conditions. This confirmed that the aging process to ensure oil wetness within the substrates was successful, and the result was used as a baseline to compare the performance of the different fluids in altering the wettability. After introducing the brine with lower salinity, as seen in Figure 7b, the contact angle increased to approximately 117° ± 2, indicating intermediate wet conditions. This confirms that traditional LSW brine had an intermediate effect on wettability but may not be enough to fully alter the wettability conditions to water wet. The contact angle was further increased to 126° ± 2 in the presence of 0.005 wt % FAU nanofluid, strongly indicating water-wet conditions that are favorable for oil recovery. The nanofluid proved successful in altering the wettability of the aged

https://dx.doi.org/10.1021/acs.energyfuels.0c02324
Energy Fuels XXXX, XXX, XXX−XXX

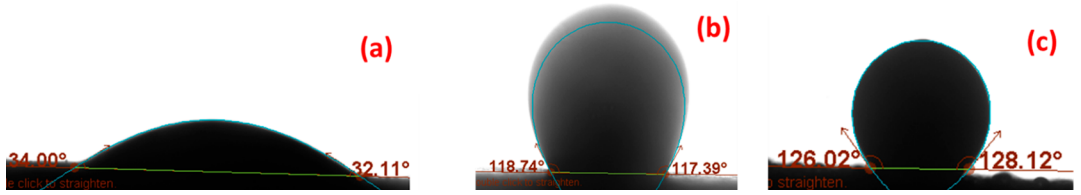

Figure 7. Contact angle measurements on chalk substrate with (a) presence of FW, (b) presence of brine with LSW 2000 ppm, and (c) treatment with 50 ppm FAU-based nanofluid.

Table 5. Austin Chalk Core Properties Used during Spontaneous Imbibition

core number	fluid	*D* (cm)	*L* (cm)	W1 (g)	W2 (g)	PV (mL)	Vb (mL)	POR %	OOIP	oil (mL)	RF	%
1	FAU-50ppm	2.54	4.0	38.70	43.49	5.09	20.25	0.25	5.09	0.65	0.128	12.80
2	LSW	2.54	3.9	38.05	42.23	4.44	19.75	0.23	4.44	0.38	0.086	8.60
3	FW	2.54	4.0	40.87	45.39	4.80	20.25	0.24	4.80	0.15	0.031	3.12

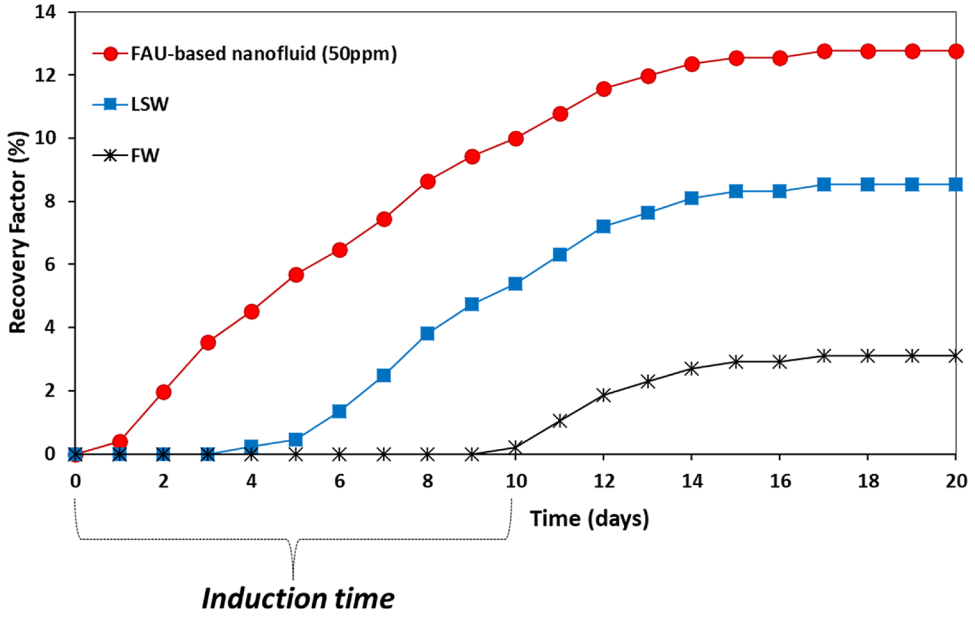

Figure 8. Imbibition of FAU-based nanofluid in comparison to LSW and FW in Austin Chalk carbonate cores at 70 °C.

substrates to strong water-wet conditions. The mechanism of wettability alteration using nanoparticles has been extensively explained in our previous works and elsewhere.[21,43]

3.5.2. Spontaneous Imbibition Tests. The second technique used to evaluate wettability alteration in the Austin Chalk core samples after contact angle measurements was a spontaneous imbibition (SI) test. The SI evaluates the ability of a wetting phase to displace a nonwetting phase under static conditions and demonstrates the influence of gravity and a capillary force.[55,56] Nanoparticles are assumed to be capable of adsorbing onto the core surface and forming a thin water-wet layer covering the oil-wet surfaces, which in theory should enhance the spontaneous imbibition of water. To evaluate the performance of the FAU nanofluid in successfully imbibing spontaneously into the rock, three imbibition experiments were conducted using three separate core plug samples. Table 5 summarizes the measured Austin Chalk core plug properties, which were used in the experiments along with the results after 20 days of spontaneous imbibition. The first two experiments conducted with FW and LSW were used as a baseline for comparison, whereas the final test was performed with the FAU-based nanofluid. The performance of the three fluids in comparison to each other is presented in Figure 8. The experiments were conducted over 20 days, and the oil recovery was reported as a function of time. On the basis of Figure 8, the poor imbibition of FW proves the oil-wet state of the carbonate cores, which was also supported by the low contact angle measurement of 33° ± 2 obtained from the substrates, as seen in Figure 7a. This low contact angle measurement results in a negative capillary pressure, which prevents water imbibition.[56] The slight oil recovery observed after 20 days was likely only due to gravitational forces. However, when using LSW, the contact angle yielded a positive capillary pressure, which resulted in approximately 8% oil recovery. However, in the presence of FAU-based nanofluids, due to positive capillary forces, water could imbibe, resulting in an increased oil recovery of 12%. Capillary forces initiated and maintained the imbibition of the FAU-nanofluid, therefore displacing oil in a countercurrent mode in which capillary and gravitational forces played a role in increasing the oil recovery.[56,57] Furthermore, the impact of the FAU-based nanofluid on wettability alteration could be further quantified by observing the decrease in the induction time. The induction time is defined as the period in which very little to no imbibition is observed. Marrow and Mason theorized that this period could be related to the time required to establish water

https://dx.doi.org/10.1021/acs.energyfuels.0c02324
Energy Fuels XXXX, XXX, XXX−XXX

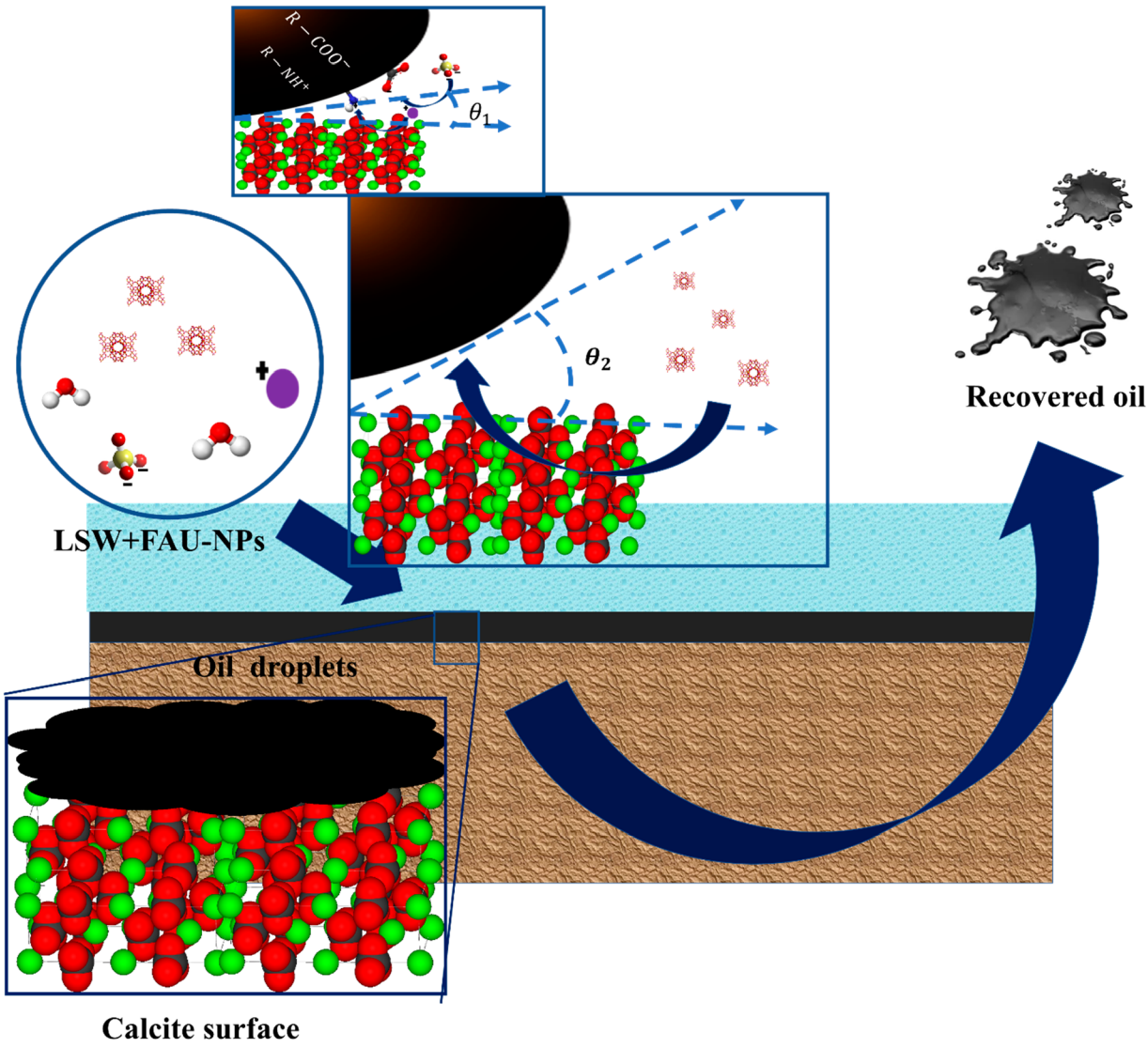

Figure 9. Schematic representation of nanoparticle ordering in the wedge film resulting in a structural disjoining pressure gradient at the wedge vertex as a result of adding FAU nanoparticles in the LSW brine.

Table 6. Oil Recovery for the Considered Flooding Scenarios

core ID	Soi (%)	Swi (%)	injected fluid	brine-flooding recovery (FW1) (%)	tertiary recovery (%)	total oil recovered (%)
1	0.84	0.16	FW	32.31	0.00	32.31
2	0.87	0.13	LSW	31.92	5.38	37.30
3	0.85	0.15	FAU	33.60	9.60	43.20

paths and/or to very slow changes in wettability resulting from the exposure of the core to brine or nanofluids.[57] The induction time decreased following the order FAU < LSW < FW. This indicates that the FAU-based nanofluid was successful in diffusing the nanoparticles into the rock, allowing more oil to detach from the surface and simultaneously altered the wettability to more water wet.

3.5.3. Mechanism of Improved Oil Recovery Using Low-Salinity Brine Coupled with FAU Nanoparticles. The mechanism behind the different effects of salinity in the presence of nanoparticles on wettability can be explained on the basis of the disjoining pressure and ζ potential.[58] According to the DLVO theory, an injection of brine with a lower salinity affects the electrostatic forces; as a result, lower salinity in the presence of nanoparticles creates a stronger thicker film, increasing the water wetness compared to with LSW alone. Moreover, the presence of LSW changes the electrostatic interactions between the fluid−fluid and the rock−fluid interfaces. Adding FAU nanoparticles increased the ζ potential to be more negative, hence increasing the electrostatic repulsive forces and making the wedge film between the surface and oil become larger. Consequently, the nanofluid spreads on the surface, and depending on their affinity with the rock surface, they detach the oil, making the surface more water wet. A summary of the mechanism involved is summarized in Figure 9.

3.6. Core-Flooding Tests. The performance of the FAU-based nanofluid in EOR from the Austin Chalk cores relative

https://dx.doi.org/10.1021/acs.energyfuels.0c02324
Energy Fuels XXXX, XXX, XXX−XXX

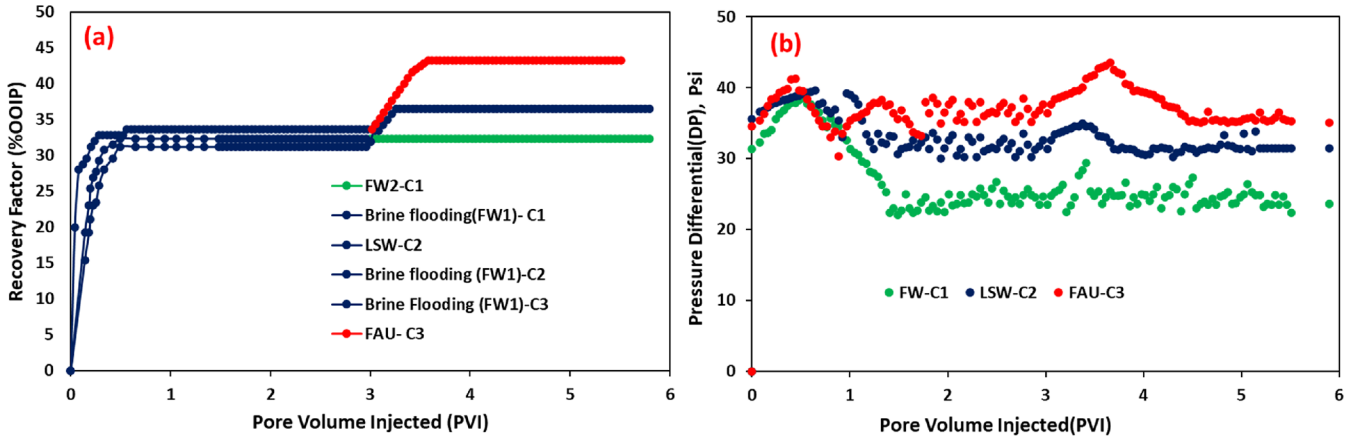

Figure 10. (a) Production profile of different injection scenarios and (b) differential pressure as a function of the pore volume.

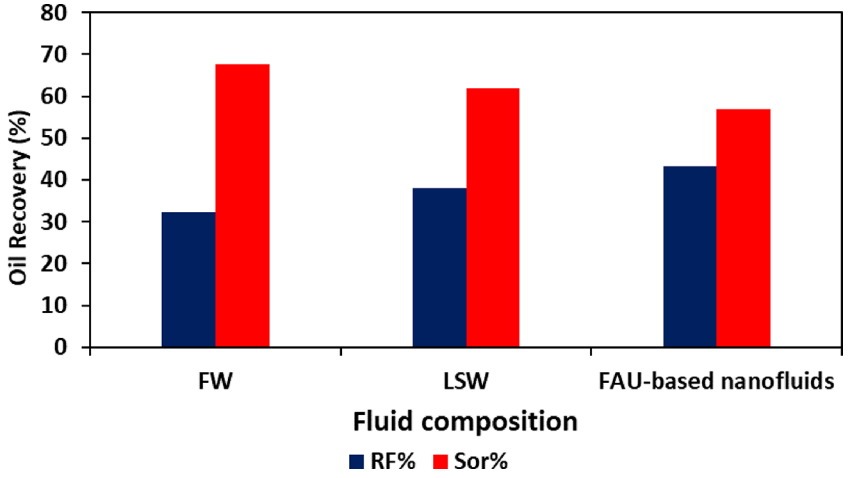

Figure 11. Residual oil saturation and total oil recovered for different injection scenarios.

to FW and LSW was investigated by conducting core-flooding experiments using three displacement tests. Three separate carbonate cores plugs were used for the displacement tests (a different set than the ones used for imbibition experiments), and their properties are summarized in Table 3. The results from the core-flooding tests are summarized in Table 6, showing the initial water saturation and initial oil in place, along with the effect of the respective injected fluids on tertiary oil recovery. Figure 10 shows the oil recovery obtained against the injected PV for the considered fluids. Brine flooding with FW could recover an average of 32.31% of OOIP in the secondary mode and no oil was recovered in the tertiary mode. The recovery obtained via FW injection is not due to wettability alteration in the rock but rather to the influence of the conventional waterflood process (secondary recovery mode). Subsequently, LSW recovered 31.92% in the secondary mode, and an additional 5.38% was obtained in the tertiary mode. This recovery during LSW injection can be attributed to the ζ potential at the rock/brine interface, which coincides with the negative ζ potential between the oil−brine interface that was also negative. According to Jackson et al.,[59] LSWF is successful only if the ζ potential at the rock/brine interface changes to become more negative when the oil−brine interface has a negative ζ potential in the formation brine, which was the case for this study. FAU-based nanofluid recovered 33.60% in the secondary mode and 9.60% at the tertiary stage. It is important to note that core samples C1−C3, exhibited different ultimate oil recoveries during FB flooding (secondary flooding mode). This can be attributed to the initial fluid saturations of the core samples, indicating that some crude oil confined in comparatively small pores or fractures may not be displaced. Although the literature data gives contradictory findings of LSW injection both for secondary and tertiary recovery modes, our results still coincide with what has been reported by other researchers.[60,61] The inconsistency in the reported findings can be generally ascribed to the different pore structure networks for different reservoir rocks, which controls the initial fluid saturation.[62] Moreover, the effect of the pore structure on a low-salinity water injection with nanoparticles is still another study that requires further investigations. Overall, these additional oil recoveries can be attributed to mostly improved disjoining pressure and ζ potential that greatly impacts the rock wettability changing from strong oil wet to stronger water wet that hence increases the microscopic displacement efficiency.

The oil recovered at the end of the flooding experiment for each fluid (RF%) and the residual oil saturation (S_{or}%) are depicted in Figure 11. It is clear that the residual oil composition decreased in the presence of LSW and significantly decreased in the presence of FAU nanoparticles. Theoretically, it can be claimed that, by adding nanoparticles to low-salinity water, the recovery performance and ability to alter the wettability of the rock can be improved, which can significantly enhance the trapped oil. However, it is important

https://dx.doi.org/10.1021/acs.energyfuels.0c02324
Energy Fuels XXXX, XXX, XXX−XXX

to note that, although a significant oil increment is noticeable at the tertiary stage using FAU-based nanofluids, still, substantial oil remains trapped due to the higher interfacial forces between oil and water due to higher capillary forces and possibly adverse mobility ratios that may cause viscous fingering.

4. CONCLUSION

In this study, FAU nanoparticles have been synthesized in-house and integrated with brine having a low ionic strength for EOR application in chalk carbonate formations. The BET analysis conducted on the FAU confirmed their high surface area to volume ratio, while the DLS confirmed their size on the nanoscale in different solutions. The ζ potential measurements at both the rock−brine and oil−brine interfaces were used to select the optimum LSW to prepare the FAU-based nanofluids. LSW with a concentration of 2000 ppm was selected to act as the dispersing medium for the FAU nanoparticles on the basis of the ζ potential measurements. FAU-based nanofluids were successful in reducing the IFT by 15% relative to LSW; however, the decrease was not significant enough to mobilize residual oil since the IFT was still greater than 0.001 dyn/cm. This was expected since the main mechanism of focus in this study was the wettability alteration and not necessarily IFT reduction solely. The contact angles in the presence of FW, LSW alone, and FAU nanofluids were measured as 33 ± 3°, 118 ± 3°, and, 127 ± 3°, respectively, confirming the wettability alteration from oil wet to stronger water wet, which was further supported by the SI tests that yielded 12% oil recovery by the FAU-based nanofluids after 20 days (a 4% increase relative to LSW alone) and greatly reduced the induction time relative to the other fluids. Finally, additional oil recovery with the FAU nanofluid was about 9.6% compared to 5.38% for LSW alone and 0% for FW at the tertiary stage. This further supported the applicability of FAU-based nanofluids as potential wettability modifiers in carbonate reservoirs.

■ ASSOCIATED CONTENT

Supporting Information

The Supporting Information is available free of charge at https://pubs.acs.org/doi/10.1021/acs.energyfuels.0c02324.

Figures of XRD spectra, viscosity of oil as a function of temperature, Austin Chalk core samples used in the study, carbonate substrates used in contact angle measurements, XRD pattern, and pore size distribution (PDF)

■ AUTHOR INFORMATION

Corresponding Author

Nashaat N. Nassar − *Department of Chemical and Petroleum Engineering, University of Calgary, Calgary T2N 1N4, Alberta, Canada;* orcid.org/0000-0001-9014-542X; Phone: +1 (403) 210-9772; Email: nassar@ucalgary.ca; Fax: +1 (403) 210-3973

Authors

Moussa Taleb − *Department of Chemical and Petroleum Engineering, University of Calgary, Calgary T2N 1N4, Alberta, Canada*

Farad Sagala − *Department of Chemical and Petroleum Engineering, University of Calgary, Calgary T2N 1N4, Alberta, Canada;* orcid.org/0000-0002-9435-3995

Afif Hethnawi − *Department of Chemical and Petroleum Engineering, University of Calgary, Calgary T2N 1N4, Alberta, Canada;* orcid.org/0000-0002-0879-6387

Complete contact information is available at: https://pubs.acs.org/10.1021/acs.energyfuels.0c02324

Notes

The authors declare no competing financial interest.

■ ACKNOWLEDGMENTS

The authors would like to gratefully acknowledge the Natural Sciences and Engineering Research Council of Canada (NSERC) and the Islamic Development Bank (IDB) for their support. Special thanks to Dr. Monica Bartolini Tiberi for providing access to the instrumentation facility for SARA analysis in the Department of Chemical and Petroleum Engineering at the University of Calgary and Dr. Christopher Deburr for providing access to the instrumentation facility for the analytical scanning electron microscope in the Geoscience Department at the University of Calgary. The authors would also like to acknowledge the use of the X-ray Diffractor at Dr. Pedro Pereira's laboratory and are grateful for the data collected by Dr. Gerardo Vitale. Also, a special acknowledgement to all members of Dr. Nassar's group for Nanotechnology Research at the University of Calgary for their help with the experimental analysis.

■ NOMENCLATURE

symbol = definition
FAU = Faujasite
BET = Bruneur−Emmett−Teller
CEOR = chemical enhanced oil recovery
DLS = dynamic light scattering
EOR = enhanced oil recovery
FW = formation water
k = permeability
LSW = low-salinity water
LSF = low-salinity flooding
IFT = interfacial tension
M = mobility ratio
Nc = capillary number
NP = nanoparticle
OOIP = original oil in place
Pc = capillary pressure
PV = pore volume
SEM = scanning electron microscopy
SI = spontaneous imbibition
STP = standard temperature and pressure
XRD = X-ray diffraction
Φ = porosity
θ = contact angle

■ REFERENCES

(1) British Petroleum. BP energy outlook 2035. *BP stats*, 2014.
(2) Matsuo, Y.; Yanagisawa, A.; Yamashita, Y. A global energy outlook to 2035 with strategic considerations for Asia and Middle East energy supply and demand interdependencies. *Energy Strategy Reviews* **2013**, *2* (1), 79−91.
(3) Donnelly, J. Comments: Peak Demand or Too Much Oil? *JPT, J. Pet. Technol.* **2017**, *69* (05), 12−12.

(4) Dorian, J. P.; Franssen, H. T.; Simbeck, D. R. Global challenges in energy. *Energy Policy* **2006**, *34* (15), 1984−1991.
(5) *IEA Bioenergy Annual Report*; International Energy Agency: Paris, France, 2009.
(6) Karimi, A.; Fakhroueian, Z.; Bahramian, A.; Pour Khiabani, N.; Darabad, J. B.; Azin, R.; Arya, S. Wettability alteration in carbonates using zirconium oxide nanofluids: EOR implications. *Energy Fuels* **2012**, *26* (2), 1028−1036.
(7) Pillai, P.; Mandal, A. Wettability modification and adsorption characteristics of imidazole-based ionic liquid on carbonate rock: Implications for enhanced oil recovery. *Energy Fuels* **2019**, *33* (2), 727−738.
(8) Fakoya, M. F.; Shah, S. N. Emergence of nanotechnology in the oil and gas industry: Emphasis on the application of silica nanoparticles. *Petroleum* **2017**, *3* (4), 391−405.
(9) Amanullah, M.; Al-Tahini, A. M. Nano-technology-its significance in smart fluid development for oil and gas field application. *SPE Saudi Arabia Section Technical Symposium*, Al-Khobar, Saudi Arabia, May 9−11,2009; Society of Petroleum Engineers, 2009.
(10) Bera, A.; Belhaj, H. Application of nanotechnology by means of nanoparticles and nanodispersions in oil recovery-A comprehensive review. *J. Nat. Gas Sci. Eng.* **2016**, *34*, 1284−1309.
(11) ShamsiJazeyi, H.; Miller, C. A.; Wong, M. S.; Tour, J. M.; Verduzco, R. Polymer-coated nanoparticles for enhanced oil recovery. *J. Appl. Polym. Sci.* **2014**, *131* (15), 40576.
(12) Fletcher, A.; Davis, J. How EOR can be transformed by nanotechnology. *SPE improved oil recovery symposium*, Tulsa, OK, April 24−28, 2010; Society of Petroleum Engineers, 2010.
(13) Cheraghian, G.; Hendraningrat, L. A review on applications of nanotechnology in the enhanced oil recovery part B: effects of nanoparticles on flooding. *Int. Nano Lett.* **2016**, *6* (1), 1−10.
(14) Hendraningrat, L.; Li, S.; Torsaeter, O. Enhancing oil recovery of low-permeability berea sandstone through optimized nanofluids concentration. *SPE enhanced oil recovery conference*, Kuala Lumpur, Malaysia, July 2−4, 2013; Society of Petroleum Engineers, 2013.
(15) Moradi, B.; Pourafshary, P.; Jalali, F.; Mohammadi, M.; Emadi, M. Experimental study of water-based nanofluid alternating gas injection as a novel enhanced oil-recovery method in oil-wet carbonate reservoirs. *J. Nat. Gas Sci. Eng.* **2015**, *27*, 64−73.
(16) Li, W.; Zhu, J.-H.; Qi, J.-H. Application of nano-nickel catalyst in the viscosity reduction of Liaohe extra-heavy oil by aqua-thermolysis. *Journal of Fuel Chemistry and Technology* **2007**, *35* (2), 176−180.
(17) Taborda, E. A.; Franco, C. A.; Ruiz, M. A.; Alvarado, V.; Cortes, F. B. Experimental and theoretical study of viscosity reduction in heavy crude oils by addition of nanoparticles. *Energy Fuels* **2017**, *31* (2), 1329−1338.
(18) Kazemzadeh, Y.; Eshraghi, S. E.; Kazemi, K.; Sourani, S.; Mehrabi, M.; Ahmadi, Y. Behavior of asphaltene adsorption onto the metal oxide nanoparticle surface and its effect on heavy oil recovery. *Ind. Eng. Chem. Res.* **2015**, *54* (1), 233−239.
(19) Nassar, N. N.; Hassan, A.; Pereira-Almao, P. Metal oxide nanoparticles for asphaltene adsorption and oxidation. *Energy Fuels* **2011**, *25* (3), 1017−1023.
(20) Mohammadi, M.; Akbari, M.; Fakhroueian, Z.; Bahramian, A.; Azin, R.; Arya, S. Inhibition of asphaltene precipitation by TiO2, SiO2, and ZrO2 nanofluids. *Energy Fuels* **2011**, *25* (7), 3150−3156.
(21) Nazari Moghaddam, R.; Bahramian, A.; Fakhroueian, Z.; Karimi, A.; Arya, S. Comparative study of using nanoparticles for enhanced oil recovery: wettability alteration of carbonate rocks. *Energy Fuels* **2015**, *29* (4), 2111−2119.
(22) Manan, M.; Farad, S.; Piroozian, A.; Esmail, M. Effects of nanoparticle types on carbon dioxide foam flooding in enhanced oil recovery. *Pet. Sci. Technol.* **2015**, *33* (12), 1286−1294.
(23) Ogolo, N.; Olafuyi, O.; Onyekonwu, M. O. Enhanced oil recovery using nanoparticles. *Society of Petroleum Engineers SPE*, Al-Khobar, Saudi Arabia, April 8−11, 2012.
(24) Sagala, F.; Hethnawi, A.; Nassar, N. N. Integrating Silicate-based Nanoparticles with Low Salinity Water Flooding for Enhanced Oil Recovery in Sandstone Reservoirs. *Ind. Eng. Chem. Res.* **2020**, *59*, 16225.
(25) Zargartalebi, M.; Kharrat, R.; Barati, N. Enhancement of surfactant flooding performance by the use of silica nanoparticles. *Fuel* **2015**, *143*, 21−27.
(26) Min, Y.; Akbulut, M.; Kristiansen, K.; Golan, Y.; Israelachvili, J. The role of interparticle and external forces in nanoparticle assembly. *Nat. Mater.* **2008**, *7*, 527−538.
(27) Bagwe, R. P.; Hilliard, L. R.; Tan, W. Surface modification of silica nanoparticles to reduce aggregation and nonspecific binding. *Langmuir* **2006**, *22* (9), 4357−4362.
(28) Timofeeva, E. V.; Gavrilov, A. N.; McCloskey, J. M.; Tolmachev, Y. V.; Sprunt, S.; Lopatina, L. M.; Selinger, J. V. Thermal conductivity and particle agglomeration in alumina nanofluids: experiment and theory. *Phys. Rev. E* **2007**, *76* (6), 061203.
(29) Katende, A.; Sagala, F. A critical review of low salinity water flooding: mechanism, laboratory and field application. *J. Mol. Liq.* **2019**, *278*, 627.
(30) Nasralla, R. A.; Alotaibi, M. B.; Nasr-El-Din, H. A. Efficiency of oil recovery by low salinity water flooding in sandstone reservoirs. *SPE Western North American Region Meeting*, Anchorage, AK, May 7−11, 2011;Society of Petroleum Engineers, 2011.
(31) Alagic, E.; Skauge, A. Combined low salinity brine injection and surfactant flooding in mixed- wet sandstone cores. *Energy Fuels* **2010**, *24* (6), 3551−3559.
(32) Shaker Shiran, B.; Skauge, A. Enhanced oil recovery (EOR) by combined low salinity water/polymer flooding. *Energy Fuels* **2013**, *27* (3), 1223−1235.
(33) Tang, G.-Q.; Morrow, N. R. Influence of brine composition and fines migration on crude oil/brine/rock interactions and oil recovery. *J. Pet. Sci. Eng.* **1999**, *24* (2−4), 99−111.
(34) Arab, D.; Pourafshary, P. Nanoparticles-assisted surface charge modification of the porous medium to treat colloidal particles migration induced by low salinity water flooding. *Colloids Surf., A* **2013**, *436*, 803−814.
(35) Mintova, S.; Gilson, J.-P.; Valtchev, V. Advances in nanosized zeolites. *Nanoscale* **2013**, *5* (15), 6693−6703.
(36) Kulprathipanja, S. *Zeolites in industrial separation and catalysis*; John Wiley & Sons, 2010.
(37) Wijayanto, T.; Kurihara, M.; Kurniawan, T.; Muraza, O. Experimental Investigation of Aluminosilicate Nanoparticles for Enhanced Recovery of Waxy Crude Oil. *Energy Fuels* **2019**, *33* (7), 6076−6082.
(38) Brady, P. V.; Morrow, N. R.; Fogden, A.; Deniz, V.; Loahardjo, N. Electrostatics and the low salinity effect in sandstone reservoirs. *Energy Fuels* **2015**, *29* (2), 666−677.
(39) Chen, T.; Chiu, M.-S.; Weng, C.-N. Derivation of the generalized Young-Laplace equation of curved interfaces in nano-scaled solids. *J. Appl. Phys.* **2006**, *100* (7), 074308.
(40) Hansen, F.; Rødsrud, G. Surface tension by pendant drop: I. A fast standard instrument using computer image analysis. *J. Colloid Interface Sci.* **1991**, *141* (1), 1−9.
(41) Alotaibi, M. B.; Azmy, R.; Nasr-El-Din, H. A. Wettability challenges in carbonate reservoirs. *SPE Improved Oil Recovery Symposium*, Tulsa, OK, April 24−28, 2010; Society of Petroleum Engineers, 2010.
(42) American Petroleum Institute. *Recommended practices for core analysis*; API Publishing Services: Washington DC, 1998.
(43) Sagala, F.; Montoya, T.; Hethnawi, A.; Vitale, G.; Nassar, N. N. Nanopyroxene-based nanofluids for enhanced oil recovery in sandstone cores at reservoir temperature. *Energy Fuels* **2019**, *33* (2), 877−890.
(44) Sagala, F.; Hethnawi, A.; Nassar, N. N. Hydroxyl-functionalized silicate-based nanofluids for enhanced oil recovery. *Fuel* **2020**, *269*, 117462.
(45) Ahmed, T. *Reservoir engineering handbook*; Gulf Professional Publishing, 2018.

https://dx.doi.org/10.1021/acs.energyfuels.0c02324
Energy Fuels XXXX, XXX, XXX−XXX

(46) Reinoso, D.; Adrover, M.; Pedernera, M. Green synthesis of nanocrystalline faujasite zeolite. *Ultrason. Sonochem.* **2018**, *42*, 303−309.
(47) Osatiashtiani, A.; Puertolas, B.; Oliveira, C. C. S.; Manayil, J. C.; Barbero, B.; Isaacs, M.; Michailof, C.; Heracleous, E.; Perez-Ramirez, J.; Lee, A. F.; Wilson, K. On the influence of Si: Al ratio and hierarchical porosity of FAU zeolites in solid acid catalysed esterification pretreatment of bio-oil. *Biomass Convers. Biorefin.* **2017**, *7* (3), 331−342.
(48) Sebakhy, K. O.; Vitale, G.; Pereira-Almao, P. Dispersed Ni-Doped Aegirine Nanocatalysts for the Selective Hydrogenation of Olefinic Molecules. *ACS Applied Nano Materials* **2018**, *1* (11), 6269−6280.
(49) Al Mahrouqi, D.; Vinogradov, J.; Jackson, M. D. Zeta potential of artificial and natural calcite in aqueous solution. *Adv. Colloid Interface Sci.* **2017**, *240*, 60−76.
(50) Mahani, H.; Keya, A. L.; Berg, S.; Nasralla, R. Electrokinetics of carbonate/brine interface in low-salinity waterflooding: Effect of brine salinity, composition, rock type, and pH on ζ-potential and a surface-complexation model. *Spe Journal* **2017**, *22* (01), 53−68.
(51) Jackson, M. D.; Vinogradov, J. Impact of wettability on laboratory measurements of streaming potential in carbonates. *Colloids Surf., A* **2012**, *393*, 86−95.
(52) Esfandyari Bayat, A.; Junin, R.; Samsuri, A.; Piroozian, A.; Hokmabadi, M. Impact of metal oxide nanoparticles on enhanced oil recovery from limestone media at several temperatures. *Energy Fuels* **2014**, *28* (10), 6255−6266.
(53) Lake, L. W. Enhanced oil recovery; Prentice Hall: Englewood Cliffs, NJ, 1989.
(54) Green, D. W.; Willhite, G. P. *Enhanced oil recovery*; Henry L. Doherty Memorial Fund of AIME, Society of Petroleum Engineers: Richardson, TX, 1998; Vol. *6*.
(55) Meng, Q.; Liu, H.; Wang, J. A critical review on fundamental mechanisms of spontaneous imbibition and the impact of boundary condition, fluid viscosity and wettability. *Advances in Geo-energy Research* **2017**, *1* (1), 1−17.
(56) Mohammed, M.; Babadagli, T. Wettability alteration: A comprehensive review of materials/methods and testing the selected ones on heavy-oil containing oil-wet systems. *Adv. Colloid Interface Sci.* **2015**, *220*, 54−77.
(57) Morrow, N. R.; Mason, G. Recovery of oil by spontaneous imbibition. *Curr. Opin. Colloid Interface Sci.* **2001**, *6* (4), 321−337.
(58) Sharma, M.; Filoco, P. Effect of brine salinity and crude-oil properties on oil recovery and residual saturations. *Spe Journal* **2000**, *5* (03), 293−300.
(59) Jackson, M. D.; Al-Mahrouqi, D.; Vinogradov, J. Zeta potential in oil-water-carbonate systems and its impact on oil recovery during controlled salinity water-flooding. *Sci. Rep.* **2016**, *6*, 37363.
(60) Nasralla, R. A.; Sergienko, E.; Masalmeh, S. K.; van der Linde, H. A.; Brussee, N. J.; Mahani, H.; Suijkerbuijk, B.; Alqarshubi, I. Demonstrating the potential of low-salinity waterflood to improve oil recovery in carbonate reservoirs by qualitative coreflood. *Abu Dhabi International Petroleum Exhibition and Conference*, Abu Dhabi, UAE, Nov 10−13, 2014; Society of Petroleum Engineers, 2014.
(61) Yousef, A. A.; Al-Saleh, S. H.; Al-Kaabi, A.; Al-Jawfi, M. S. Laboratory investigation of the impact of injection-water salinity and ionic content on oil recovery from carbonate reservoirs. *SPE Reservoir Evaluation & Engineering* **2011**, *14* (05), 578−593.
(62) Salathiel, R. Oil recovery by surface film drainage in mixed-wettability rocks. *JPT, J. Pet. Technol.* **1973**, *25* (10), 1216−1224.

https://dx.doi.org/10.1021/acs.energyfuels.0c02324
Energy Fuels XXXX, XXX, XXX−XXX